PAPER • OPEN ACCESS

Collection efficiencies of ionization chambers in pulsed radiation beams: an exact solution of an ion recombination model including free electron effects

To cite this article: John D Fenwick and Sudhir Kumar 2023 *Phys. Med. Biol.* **68** 015016

IOP Publishing Phys. Med. Biol. 68 (2023) 015016 https://doi.org/10.1088/1361-6560/aca74e

Physics in Medicine & Biology

IPEM Institute of Physics and Engineering in Medicine

OPEN ACCESS

RECEIVED
28 July 2022

REVISED
21 November 2022

ACCEPTED FOR PUBLICATION
29 November 2022

PUBLISHED
26 December 2022

PAPER

Collection efficiencies of ionization chambers in pulsed radiation beams: an exact solution of an ion recombination model including free electron effects

John D Fenwick[1,*] **and Sudhir Kumar**[2]

[1] Department of Molecular and Clinical Cancer Medicine, Institute of Systems, Molecular and Integrative Biology, University of Liverpool, The Sherrington Building, Ashton Street, Liverpool L69 3BX, United Kingdom

[2] Radiological Physics and Advisory Division, Bhabha Atomic Research Centre, CT & CRS Building, Anushaktinagar, Mumbai-400094, India

[*] Author to whom any correspondence should be addressed.

E-mail: john.fenwick@liverpool.ac.uk

Keywords: ionisation chamber, ion recombination, dose-per-pulse, collection efficiency, free electrons

Abstract

Objective. Boag *et al* (1996) formulated a key model of collection efficiency for ionization chambers in pulsed radiation beams, in which some free electrons form negatively charged ions with a density that initially varies exponentially across the chamber. This non-uniform density complicates ion recombination calculations, in comparison with Boag's 1950 work in which a collection efficiency formula, f, was straightforwardly obtained assuming a uniform negative ion cloud. Boag *et al* (1996) therefore derived collection efficiency formulae f', f'' and f''' based on three approximate descriptions of the exponentially-varying negative ion cloud, each uniform within a region. Collection efficiencies calculated by Boag *et al* (1996) using these formulae differed by a maximum of 5.1% relative (at 144 mGy dose-per-pulse with 212 V applied over a 1 mm electrode separation) and all three formulae are often used together. Here an exact solution of the exponentially-varying model is obtained. *Approach.* The exact solution was derived from a differential equation relating the number of negative ions collected from within some distance of the anode to numbers of ions initially located within that region. Using the resulting formula, f_{exp}, collection efficiencies were calculated for a range of ionization chamber properties and doses-per-pulse, and compared with f, f', f'' and f''' values and results from an ion transport code. *Main results.* f_{exp} values agreed to 5 decimal places with ion transport code results. The maximum relative difference between f_{exp} and f''', which was often closest to f_{exp}, was 0.78% for the chamber properties and doses-per-pulse studied by Boag *et al* (1996), rising to 6.1% at 1 Gy dose-per-pulse and 2 mm electrode separation. *Significance.* Use of f_{exp} should reduce ambiguities in collection efficiencies calculated using the approximate formulae, although like them f_{exp} does not account for electric field distortion, which becomes substantial at doses-per-pulse $\geqslant$100 mGy.

1. Introduction

Ion recombination effects in radiotherapy dosimetry are currently receiving much attention, stemming from increased doses-per-pulse of around 0.8 mGy in photon beams generated by flattening filter-free linear accelerators (linacs), 10–100 mGy in electron beams used intra-operatively, and 10–5000 mGy in FLASH radiotherapy treatments, in comparison to around 0.3 mGy in conventional photon beams generated by linacs with flattening filters (Di Martino *et al* 2005, Laitano *et al* 2006, Christensen *et al* 2016, Petersson *et al* 2017, Gotz *et al* 2017, McManus *et al* 2020 and Kranzer *et al* 2021).

Recombination can be classified as *initial*, between charge carriers generated within a single ion track (Jaffé 1913, 1929), and *volume*, between carriers from different ion tracks (Thomson and Thomson 1928). In

photon and electron beams initial recombination (sometimes called columnar recombination) is usually ignored, with volume (or general) recombination considered to be the dominant process (Christensen *et al* 2016). In these beams a pulse of radiation initially liberates free electrons and positive ions, and within the sensitive volume of an ionization chamber the free electrons drift rapidly towards the anode. In fact, compared to the positive ions the electrons move sufficiently fast that they are often all considered to have either reached the anode or formed negative ions by becoming attached to oxygen molecules, before the positive ions have moved from the locations in which they were created. After this early phase the positive and negative ions drift past each other more slowly, reaching the electrodes or recombining. To minimize recombination, distances d between electrodes are limited to millimetres over which potential differences V of hundreds of volts are applied to generate high electric fields.

Boag *et al* (1996) formulated a landmark model of ion recombination for parallel plate ionization chambers in pulsed radiation beams (Kranzer *et al* 2021). In an earlier publication Boag (1950) had assumed that free electrons liberated in the chamber volume travel negligible distances before forming a uniform cloud of negative ions that drifts slowly through the uniform cloud of positive ions moving in the opposite direction. But in the 1996 study Boag *et al* instead took the free electrons to have a probability exp(-as) of rapidly drifting a distance s or more through air before becoming attached to oxygen. Correspondingly, a fraction

$$p = (1 - \exp(-ad))/(ad), \tag{1}$$

of the free electrons were expected to be collected at the anode and the rest to form negative ions with a number density

$$n_-(x, t = 0) = n_0(1 - \exp(-ax)). \tag{2}$$

In these equations n_0 is the uniform number density of positive ions (or electrons) originally liberated by the radiation pulse; x is the distance from the cathode; $t = 0$ denotes an early time before the ions have moved significantly; and a depends on the electrical field strength and properties of air filling the detector sensitive volume (Thomson and Thomson 1928). Throughout the rest of this work number (not charge) density is succinctly referred to as 'density'.

The total number of recombinations that occur when uniform clouds of positive and negative ions drift past each other can be calculated straightforwardly enough, because the resulting recombination rates are also uniform throughout the overlapping region (Boag *et al* 1996). However, when the negatively charged cloud is initially non-uniform, recombination rates vary throughout the overlap, causing the positive ion cloud also to become non-uniform and making the number of recombinations more difficult to determine. As a result, Boag *et al* (1996) obtained three approximate formulae f', f'' and f''' for ionization chamber collection efficiency, defined as the ratio of the charge collected by a chamber to the charge liberated in its sensitive volume. The formulae are based on three uniform approximations to the non-uniform initial negative ion density of equation (2): n_-', a uniform density $(1 - p)n_0$ extending from one electrode to the other; n_-'', a uniform density n_0 extending from $x = pd$ to d; and n_-''', a uniform density $(1 - \lambda)n_0$ extending from λd to d where $\lambda = 1 - \sqrt{1 - p}$ (figure 1). The resulting approximate collection efficiency formulae differ from each other and from the earlier formula f obtained by Boag (1950) which ignored free electron effects.

Boag *et al* (1996) expected that f''' would be more accurate than f'' and f'' than f', because approximations n_-', n_-'' and n_-''' visually appear to provide incrementally improving descriptions of the exponential variation of ion density with x (figure 1). However, collection efficiency calculations continue to be made using all three approximate formulae (Laitano *et al* 2006, Christensen *et al* 2016, Gotz *et al* 2017, McManus *et al* 2020) and f' has also been used alone due to its algebraic properties (Di Martino *et al* 2005).

In fact, it is possible to obtain an analytical solution for recombination given the initial exponential distribution of negative ions described in equation (2), as set out in the appendix. This leads to an exact collection efficiency formula f_{exp}, which can be used to determine the relative accuracies of the approximate formulae of Boag *et al* (1996) and which potentially removes the need to make three different approximate calculations of collection efficiency. It should be noted, though, that the model formulated by Boag *et al* does not account for distortion of the applied electrical field by charge imbalance. Consequently, neither the exact f_{exp} formula nor any of the approximate formulae account for such distortions. These become substantial at very high doses-per-pulse, one hundred mGy or higher (Boag *et al* 1996), and are greater at chamber voltages $\geqslant$150 V due to increasing numbers of free electrons reaching the anode (Gotz *et al* 2017, Petersson *et al* 2017).

In the main body of this work the collection efficiency formula f_{exp} is set out alongside the approximate formulae of Boag *et al* (1996) and the original 1950 Boag formula. Collection efficiency values calculated using all the formulae are compared in tables and graphs. Details are also provided of a one-dimensional numerical scheme for calculating ion transport, recombination and collection efficiency, which was used to check the correctness of f_{exp} whose derivation is lengthy.

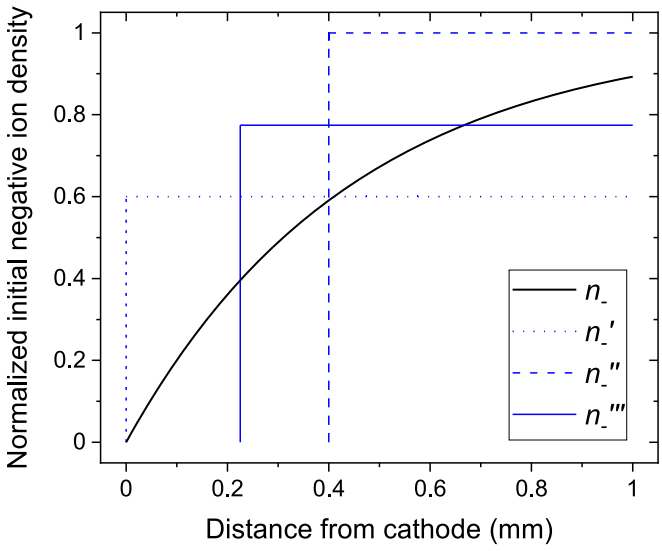

Figure 1. A plot of the initial, $t = 0$, density n_- of negative ions versus distance from the cathode in the sensitive volume of an ionization chamber, according to the model of Boag *et al* (1996) allowing for free electron effects. Density has been normalized to the initial uniform density of positive ions, n_0, and is plotted for a chamber with a 1 mm distance between electrodes in which 40% of free electrons are collected and 60% form the negative ions. Also plotted normalized to n_0 are the approximate density distributions n_-', n_-'' and n_-''' used to derive the collection efficiency formulae f', f'' and f''' of Boag *et al* (1996).

2. Materials and methods

2.1. Nomenclature

Quantities appearing outside the derivation of f_{exp} presented in section 2.2 and the appendix are denoted by the following symbols –

$f, f', f'', f''', f_{\text{exp}}$, ionization chamber collection efficiency formulae
p, fraction of free electrons collected at the anode
d, electrode spacing
a, drift coefficient for free electrons
γ, rate-constant for attachment of free electrons to oxygen
n_0, initial uniform density of positive ions or free electrons
$n_\pm$, density distributions of positive and negative ions
n_-', n_-'', n_-''', approximations to n_- at $t = 0$ used to derive f', f'' and f'''
V, potential difference across the chamber
k_1, k_2, k_e, mobilities of positive and negative ions and electrons
v_+, v_-, v_e, drift velocities of positive and negative ions and electrons
α, rate-constant for recombination between positive and negative ions
$u = \frac{n_0 \alpha d^2}{(k_1 + k_2)V}$, dimensionless combination of parameters

Notice that the composite parameter u varies with n_0 and thus with dose-per-pulse. For ease of reference the symbols used to represent quantities that appear in Boag *et al* (1996) are nearly identical to those in the 1996 publication. Quantities used only in the derivation of f_{exp} are described as they are introduced.

2.2. Derivation of f_{exp}

The derivation is set out in the appendix and has two key steps. First, the number of negative ions initially located in a thin slab lying a distance x from the cathode that eventually recombine with positive ions is related to N_{+x}, the total number of positive ions through which the slab of negative ions passes on its way to the anode (equation (A6)). This step achieves little on its own since N_{+x} is not known *ab initio*. However, at the second step it is recognized that N_{+x} is equal to $N_+(x,\ t\ =\ 0)$, the known total number of positive ions initially lying between the slab and the anode immediately after the radiation pulse, minus $\tilde{R}_x$, the number of these positive ions that have recombined with negative ions before the slab passes through them (equation (A10)). By definition, $\tilde{R}_x$ is also equal to the integral of all the negative ions lying in thin slabs initially located $> x$ from the cathode that have recombined with positive ions en route to the anode.

These considerations allow a differential equation (A15) to be constructed that links the total number of negative ions eventually reaching the anode to quantities related to the known initial density distributions of positive and negative ions. This equation is solved to obtain a formula for the total number of negative ions

Table 1. Ionization chamber parameter values used in collection efficiency calculations that are not based directly on u and p.

Parameter	Value[a]
α	1.3×10^{-12} m^3 s^{-1}
k_1	1.87×10^{-4} m^2 V^{-1} s^{-1}
k_2	2.09×10^{-4} m^2 V^{-1} s^{-1}
k_e	0.083 m^2 V^{-1} s^{-1}
γ	$[1.1 + 11.3 \times \exp(-1.04 \times 10^{-5} \times E^{b)}] \times 107$ s^{-1} for $E \geqslant 10^5$ V m^{-1}
	9.0×10^7 s^{-1} for $E = 5 \times 10^4$ V m^{-1}
n_0-per-Gy	2.216×10^{17} m^{-3} Gy^{-1}
d	10^{-3} m (Advanced Markus), 2×10^{-3} m (classic Markus)

[a] All values derived from Gotz *et al* (2013) except for n_0-per-Gy which follows directly from (W/e) and the density of dry air at 20°C and 101.325 kPa.

[b] E is electric field-strength measured in V m^{-1}, equal to the applied potential difference divided by the electrode separation.

collected, expressed in terms of an integral of a function $g(x)$ related to the initial ion density distributions (equation (A22)). For a uniform initial positive ion distribution and the exponential negative ion distribution of equation (2), f_{exp} can then be obtained in closed form from equation (A22).

In fact, the same process can be followed up to equation (A22) for any positive and negative ion distributions, with different distributions leading to different $g(x)$ functions. Analytical collection efficiency formulae can then be obtained for those distributions that yield $g(x)$ functions with closed form integrals, while for other distributions collection efficiencies can be calculated by numerical integration of equation (A22), a faster method than numerical simulation of the whole ion transport, recombination and collection process.

2.3. Collection efficiency calculations

Three sets of calculations have been performed. First, using the f_{exp} formula collection efficiencies were calculated directly for generic ionization chambers with the same set of u and p values for which Boag *et al* (1996) compiled f, f', f'' and f''' values in their table 1. It is easy to evaluate f_{exp} using a pocket calculator, given values of the exponential integral function which can be obtained from tables or online resources (e.g. Casio's *Keisan* site). However, exponential integral values can also be obtained using functions available in languages such as MATLAB (Mathworks, Natick, MA) and *R* (R Foundation, Vienna, Austria). And since the collection efficiency formulae were evalulated many times in this work, code was written in *R* version 4.0.2 to repeatedly and rapidly compute them.

Using all five formulae a second set of collection efficiencies was calculated for chambers with the specific properties listed in table 1. The tabulated parameter values describe properties of air and the widths of the gaps between the parallel plate electrodes in the dosimeters being studied, namely 1 mm representing an Advanced Markus chamber (PTW 34045, Freiburg, Germany) and 2 mm representing the classic Markus chamber (PTW 23343) and also the Roos (PTW 34001), NACP Plane Parallel (IBA, Louvain-la-Neuve, Belgium) and Exradin A10 (Standard Imaging, Madison WI) chambers. Calculations were carried out for doses-per-pulse of 1, 10, 100 and 1000 mGy and chamber voltages across the range 100–1000 V.

The air-related parameter values in table 1 were taken from Gotz *et al* (2017), except for the n_0-per-Gy factor which was obtained from the (W/e) value of 33.97 eV required to generate each electron/ion pair in dry air (Boutillon and Perroche-Roux 1987) and the 1.204 kg m^{-3} density of dry air at 20°C temperature and 101.325 kPa pressure. The tabulated k_e value was estimated from figure 2(a) of Gotz *et al* (2017), while the γ function describing the electron attachment rate-constant and its dependence on electric field-strength was obtained by fitting data plotted in figure 2(b) of the same publication. The drift coefficient for free electrons, a, was calculated from γ using $a = (\gamma/v_e)$ where $v_e = k_e(V/d)$ is the electron drift velocity. The relationship between a and γ follows because these coefficients are the constants of proportionality linking free electron density to its rates of loss with distance travelled and time respectively (Boag *et al* 1996, Gotz *et al* 2017). Next, p was calculated from the values of a and d via equation (1). Then u values were calculated from α, d, k_1 and k_2 plus the chamber voltage and initial ion density, n_0, which was obtained from the dose-per-pulse and the n_0-per-Gy factor in table 1. Finally, ionization chamber collection efficiencies were calculated for these u, p and (ad) values.

In a third set of calculations the transport of positive and negative ions towards the cathode and anode was computed using a one-dimensional numerical scheme, starting from a uniform positive charge cloud and the distribution of negative ions described by equation (2). The positive and negative ion drift velocities v_+ and v_- were determined from the ion mobilities and electric field-strength (V/d), and transport calculations were carried out in a rest-frame in which the negative ions were static and the positive ions moved past them with a

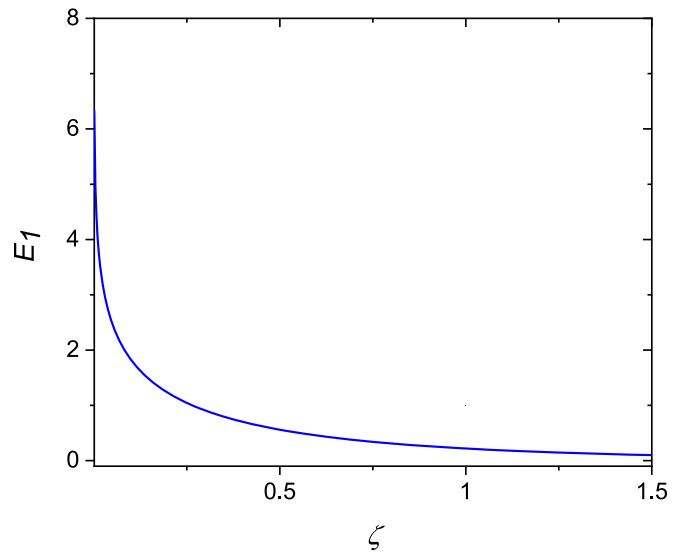

Figure 2. The exponential integral function $E_1(\zeta)$ graphed over the range $\zeta = 10^{-3}$ to 1.5. E_1 tends to infinity as ζ approaches zero.

velocity $(\nu_+ + \nu_-) = (k_1 + k_2)(V/d)$. This is the reverse of the rest-frame used in the derivation of the f_{exp} formula, in which the positive ions were stationary (see appendix).

To travel right through the negative ion cloud, positive ions need to move a maximum of 1 mm in the chosen rest-frame. This movement was computed in 5×10^4 steps, equivalent to a distance-per-step of 20 nm, and ion number densities were discretized in corresponding 20 nm bins. At each step the positive ion density distribution was shifted 20 nm through the negative ion distribution, and recombination during the step was accounted for by depleting the densities of positive and negative ions within each bin by $\alpha n_+ n_- \Delta t$ where Δt is the time-interval between steps, equal to $2 \times 10^{-8}/(\nu_+ + \nu_-)$ or 1.68×10^{-10} s. Finally, the collection efficiency was determined by summing the numbers of positive ions in bins emerging from the cathode side of the negative ion cloud and dividing by the initial total number of positive ions.

This scheme provides a check of the f_{exp} formula, and was used to independently compute collection efficiencies for the generic chamber with $u = 0.5$ and $p = 0.1$, 0.3 and 0.6. These values were chosen because collection efficiencies calculated by Boag *et al* (1996) for $u = 0.5$ differed substantially from one and varied notably with p. So far as possible the parameter values of table 1 were used in the numerical calculations. However, for p to equal 0.1, 0.3 and 0.6, the product (ad) had to be set to 10.0000, 3.1971 and 1.1263 respectively rather than being computed from γ, k_e, V and d. To achieve the u value of 0.5 at a chamber voltage of 300 V, n_0 was set to $9.138\,46 \times 10^{16}$ m^{-3} equivalent to a dose-per-pulse of 41.3 mGy, rather than being calculated for a pre-specified dose-per-pulse.

3. Results

3.1. The f_{exp} formula

The collection efficiency formula derived analytically in the appendix is

$$f_{exp} = \frac{1}{u} \ln(\, 1 + R \exp(R)[\, E_1(R \exp(-ad)) - E_1(R)\,]\,), \tag{3}$$

where $R = u/(ad)$ and E_1 is the exponential integral function (Gradshteyn and Ryzhik 2007). Alternatively, f_{exp} can be written as

$$f_{exp} = \frac{1}{u} \ln(\, 1 + u\, h(u, ad)), \tag{4}$$

where

$$h(u, ad) = \frac{1}{ad} \exp\left(\frac{u}{ad}\right)\left[E_1\left(\frac{u}{ad} \exp(-ad)\right) - E_1\left(\frac{u}{ad}\right)\right]. \tag{5}$$

For comparison, the formulae obtained by Boag (1950) and Boag *et al* (1996) are

$$f = \frac{1}{u}\ln(1+u) \tag{6}$$

$$f' = \frac{1}{u}\ln\left(1+u\left(\frac{\exp(pu)-1}{pu}\right)\right) \tag{7}$$

$$f'' = p + \frac{1}{u}\ln(1+u(1-p)) \tag{8}$$

$$f''' = \lambda + \frac{1}{u}\ln\left(1+u\left(\frac{\exp(\lambda(1-\lambda)u)-1}{\lambda u}\right)\right). \tag{9}$$

where $\lambda = 1 - \sqrt{1-p}$.

Whereas the collection efficiency formula f ignores free electron effects and is determined by u alone, f', f'' and f''' approximately account for these effects and depend on both u and p. At first sight f_{exp} appears to depend on u and (ad) instead. However, p and (ad) are determined uniquely by each other (equation (1)) and therefore f_{exp} can equivalently be viewed as being determined by u and p.

The exponential integral function E_1 in equation (3) is defined as

$$E_1(\zeta) = \int_{\zeta}^{\infty} \frac{\exp(-\zeta')}{\zeta'} d\zeta', \tag{10}$$

and has the widely tabulated form shown in figure 2. A difference between two E_1 values also appears in a collection efficiency formula obtained by Jaffé for ion tracks that run parallel to the electric field in an ionization chamber, based on his theory of initial recombination (Jaffé 1913, Jaffé 1929, Kanne and Bearden 1936, Christensen *et al* 2016).

3.2. Variation of f_{exp} with u and p for generic chambers

Table 2 shows collection efficiencies calculated by Boag *et al* (1996) using the f, f', f'' and f''' formulae for generic ionization chambers having a range of (u, p) values, together with corresponding collection efficiencies calculated using f_{exp}. When determining f_{exp}, values of (ad) corresponding to the values of p were first obtained by numerically inverting equation (1) and were then used alongside u in equation (3).

Across all the (u, p) combinations values of f, f', f'' and f''' have the consistent order $f'' > f''' > f' > f$. The maximum relative difference between f', f'' and f''' values is 5.1%, seen at $u = 0.5$ with $p = 0.5$, equivalent to 144 mGy per pulse with 212 V applied over an electrode gap of 1 mm. Boag *et al* (1996) expected f''' to be the most accurate of the approximate formula, and f''' values do indeed lie closest to the exact f_{exp} values over the range $p = 0.3$–0.6. However, for p values of 0.1–0.2, f'' lies closer to f_{exp}. The greatest difference between f''' and f_{exp} values is seen at $u = 0.5$ with $p = 0.2$, where $f''' = 0.8596$ and $f_{exp} = 0.8663$. The correction factors corresponding to these collection efficiencies are 1.163 and 1.154 which differ by 0.78% relative.

To make the tabulated values of p more tangible, the electrode separation d to which each p value corresponds has been calculated by dividing the equivalent (ad) value by a, which in turn was calculated from γ, k_e and the electric field strength (V/d). These d values are shown in table 2 for field strengths of 100 and 300 V mm^{-1}. Similarly, doses-per-pulse corresponding to the tabulated levels of u have been calculated using the k_1, k_2, α and n_0-per-Gy values listed in table 1, assuming applied potential differences of 100 and 300 V and electrode separations of 1 and 2 mm. The dose-per-pulse values are listed in table 3.

Values of the $h(u, ad)$ (or equivalently $h(u, p)$) term of equation (4) are shown in table 4 for the same (u, p) combinations for which collection efficiencies are listed in table 2. The degree to which h exceeds one is a measure of the effect of free electrons on collection efficiency, since when h equals one the f_{exp} formula reduces to f. Across all the (u, p) combinations h varies between 1.0011 and 1.1987, exceeding 1.10 for $u = 0.3$ and $p \geqslant 0.5$, and for $u = 0.5$ and $p \geqslant 0.3$.

3.3. Variation of f_{exp} with voltage and dose-per-pulse for Advanced and classic Markus chambers

Figure 3 shows Jaffé plots describing the variation of (1/collection efficiency) with $(1/V)$ for a parallel plate ionization chamber with the air-related properties listed in table 1 and the 1 mm electrode separation of the Advanced Markus chamber. The figure comprises four graphs showing results for doses-per-pulse of 1, 10, 100 and 1000 mGy. Each graph includes lines representing collection efficiencies calculated across a potential difference range of 100–1000 V according to the f_{exp}, f, f', f'' and f''' formulae. Collection efficiency values have the consistent order $f'' > f''' > f''' >$ f, the same pattern seen in table 2. To assist further comparisons with the results shown in table 2 it is useful to note that for the 1 mm electrode gap, chamber voltages of 100, 200 and 300 V correspond to p values of 0.163, 0.515 and 0.738, and to u values of 7.275, 3.638 and 2.425 when the dose-per-pulse is 1 Gy, u scaling linearly with dose-per-pulse.

Table 2. Ionization chamber collection efficiencies calculated for sensitive volumes with various u and p values and corresponding (ad) and d values. The collection efficiencies have been computed according to Boag's original formula f which ignores the collection of free electrons, the formulae f', f'' and f''' obtained for uniform approximations to the exponential distribution of negative ions described by equation (2), and f_{exp} obtained exactly for the exponential distribution.

$p = 0$		$p =$	0.1	0.2	0.3	0.4	0.5	0.6
$(ad) = \infty$		$(ad) =$	10.0000	4.9651	3.1971	2.2317	1.5936	1.1263
[b] d_{100} (mm) $= \infty$		d_{100} (mm) $=$	1.6	0.8	0.5	0.4	0.3	0.2
[b] d_{300} (mm) $= \infty$		d_{300} (mm) $=$	15.6	7.7	5.0	3.5	2.5	1.8
$u = 0.01$	$f = 0.9950$	$f' =$	0.9955	0.9960	0.9965	0.9970	0.9975	0.9980
		$f'' =$	0.9960	0.9968	0.9976	0.9982	0.9988	0.9992
		$f''' =$	0.9958	0.9964	0.9971	0.9977	0.9982	0.9987
		$f_{exp} =$	0.9959	0.9966	0.9972	0.9977	0.9982	0.9986
0.03	$f = 0.9853$	$f' =$	0.9868	0.9882	0.9897	0.9911	0.9926	0.9941
		$f'' =$	0.9881	0.9906	0.9928	0.9947	0.9963	0.9976
		$f''' =$	0.9874	0.9894	0.9913	0.9931	0.9948	0.9962
		$f_{exp} =$	0.9879	0.9900	0.9917	0.9932	0.9945	0.9957
0.10	$f = 0.9531$	$f' =$	0.9577	0.9622	0.9669	0.9715	0.9762	0.9809
		$f'' =$	0.9618	0.9696	0.9766	0.9827	0.9879	0.9922
		$f''' =$	0.9598[a]	0.9661	0.9721	0.9778	0.9830	0.9878
		$f_{exp} =$	0.9613	0.9679	0.9732	0.9779	0.9821	0.9861
0.30	$f = 0.8745$	$f' =$	0.8862	0.8980	0.9100	0.9223	0.9347	0.9473
		$f'' =$	0.8967	0.9170	0.9354	0.9517	0.9659	0.9778
		$f''' =$	0.8916	0.9080	0.9237	0.9386	0.9526	0.9656
		$f_{exp} =$	0.8955	0.9125	0.9266	0.9390	0.9504	0.9610
0.50	$f = 0.8109$	$f' =$	0.8278	0.8451	0.8628	0.8810	0.8997	0.9188
		$f'' =$	0.8431	0.8729	0.9002	0.9247	0.9463	0.9646
		$f''' =$	0.8356	0.8596	0.8828	0.9051	0.9262	0.9459
		$f_{exp} =$	0.8414	0.8663	0.8872	0.9057	0.9229	0.9392

[a] The listed value is fractionally lower than the figure of 0.9600 in table 1 of Boag *et al* (1996) because a computational check indicated a value of 0.959 77. Checks of all the other f, f', f'' and f''' values agreed with the original tabulation.

[b] d_{100} and d_{300} are the electrode separations that correspond to the tabulated (ad) value for an electrical field within the chamber of 100 and 300 V mm^{-1} respectively.

Table 3. Doses-per-pulse (dpp) corresponding to the u values of tables 2 and 3, calculated for applied potential differences of 100 and 300 V, and electrode separations of 1 and 2 mm.

u	dpp (100 V, 1 mm) (mGy)	dpp (100 V, 2 mm) (mGy)	dpp (300 V, 1 mm) (mGy)	dpp (300 V, 2 mm) (mGy)
0.01	1.4	0.3	4.1	1.0
0.03	4.1	1.0	12.4	3.1
0.10	13.8	3.4	41.3	10.3
0.30	41.3	10.3	123.9	31.0
0.50	68.9	17.2	206.6	51.7

Table 4. Values of the h term of equation (4) listed for the same set of u and p values that appear in table 2.

u	$h(u, p = 0.1)$	$h(u, p = 0.2)$	$h(u, p = 0.3)$	$h(u, p = 0.4)$	$h(u, p = 0.5)$	$h(u, p = 0.6)$
0.01	1.0011	1.0020	1.0027	1.0033	1.0039	1.0044
0.03	1.0032	1.0048	1.0078	1.0098	1.0113	1.0129
0.10	1.0105	1.0189	1.0258	1.0318	1.0372	1.0424
0.30	1.0293	1.0533	1.0734	1.0911	1.1075	1.1228
0.50	1.0461	1.0842	1.1167	1.1456	1.1728	1.1987

Plots of $(1/f)$ are roughly linear in figure 3, whereas the $(1/f_{exp})$, $(1/f')$, $(1/f'')$, and $(1/f''')$ plots initially curve upwards before also rising approximately linearly. The f''' and f'' curves lie closer to f_{exp} than do f or f'. Generally f''' is closer to f_{exp} than is f'', but at 100 V (corresponding to $p = 0.1633$) f'' is closer to f_{exp}. The $(1/f_{exp})$ and $(1/f''')$

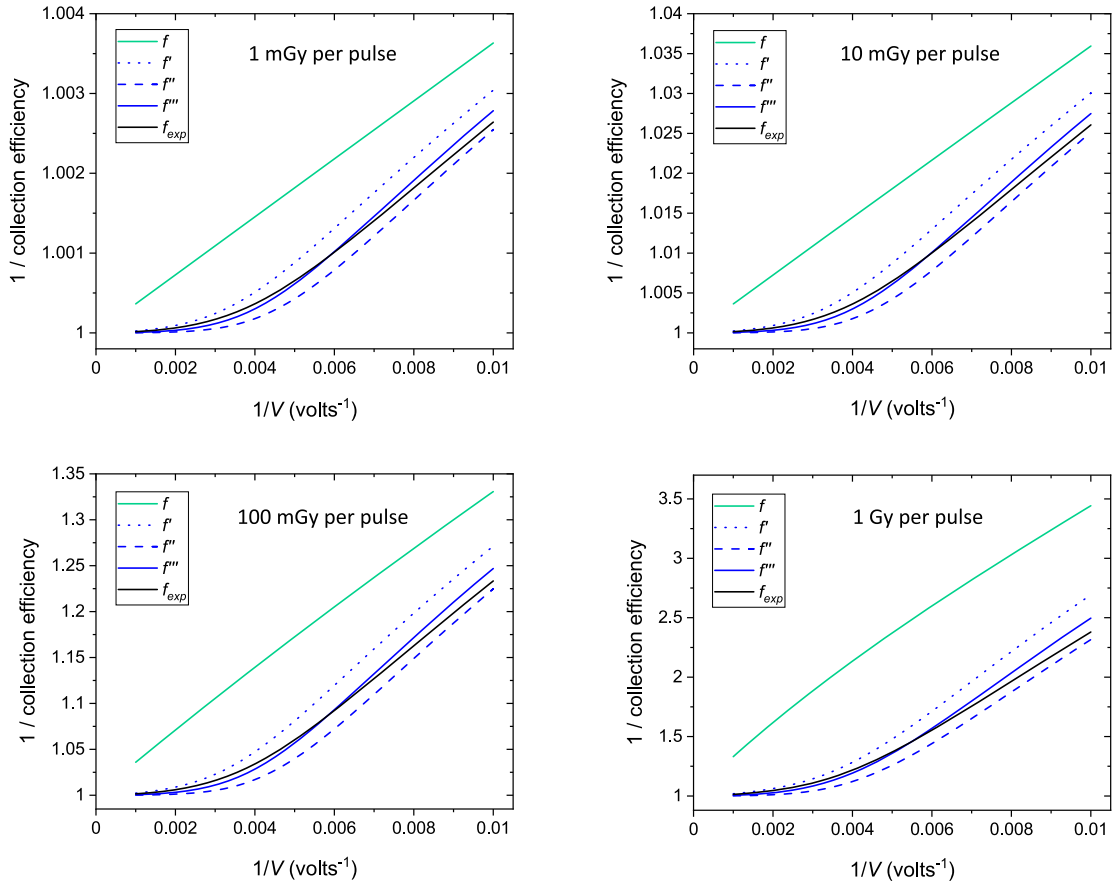

Figure 3. Jaffé plots of (1/collection efficiency) versus (1/V) calculated for a parallel plate ionization chamber with the air-related properties listed in table 1 and a 1 mm gap between electrodes. Results are shown for voltages in the range 100–1000 V, and for doses-per-pulse of 1, 10, 100 and 1000 mGy.

curves cross in each graph, ($1/f'''$) lying below ($1/f_{\text{exp}}$) at higher voltages and above it at lower ones. At doses-per-pulse of 1, 10, 100 and 1000 mGy maximum relative differences between ($1/f'''$) and ($1/f_{\text{exp}}$) are 0.014%, 0.14%, 1.1% and 4.9%.

Figure 4 shows corresponding Jaffé plots for detectors with an electrode separation of 2 mm, for example the classic Markus and NACP Plane Parallel chambers. Collection efficiencies are substantially lower (higher reciprocals) for this separation, because the ions have further to travel to reach the electrodes and they drift more slowly since the same applied voltage produces a weaker electric field. When comparing these collection efficiencies with those of table 2, chamber voltages of 100, 200 and 300 V correspond to p values of 0.027, 0.082 and 0.179 for the 2 mm electrode gap, and to u values of 29.100, 14.550 and 9.700 when the dose-per-pulse is 1 Gy.

Plot lines in figure 4 describing ($1/f''$) and ($1/f'''$) are again closer to ($1/f_{\text{exp}}$) than are ($1/f'$) lines. While f''' is closer than f'' to f_{exp} at high chamber voltages, f'' values are closest to f_{exp} at 100–200 V ($p = 0.027$–0.082). At doses-per-pulse of 1, 10, 100 and 1000 mGy maximum relative differences between($1/f''$) and ($1/f_{\text{exp}}$) are 0.022%, 0.21%, 1.5% and 6.1%.

3.4. Computational check of the f_{exp} formula

The numerical scheme for calculating ion transport and recombination described in the *Materials and methods* was used to check three of the f_{exp} values calculated for the generic ionization chamber. The scheme was run with parameters mostly set to the values in table 1 but with free electron transport adjusted to achieve p values of 0.1, 0.3 and 0.6, and with the dose-per-pulse selected as 41.2 mGy to achieve a u value of 0.5. The computed collection efficiencies were 0.841 41, 0.887 18 and 0.939 17 for the 0.1, 0.3 and 0.6 values of p respectively, in agreement to 5 decimal places with collection efficiencies calculated from the f_{exp} formula and shown to 4 decimal places in table 2.

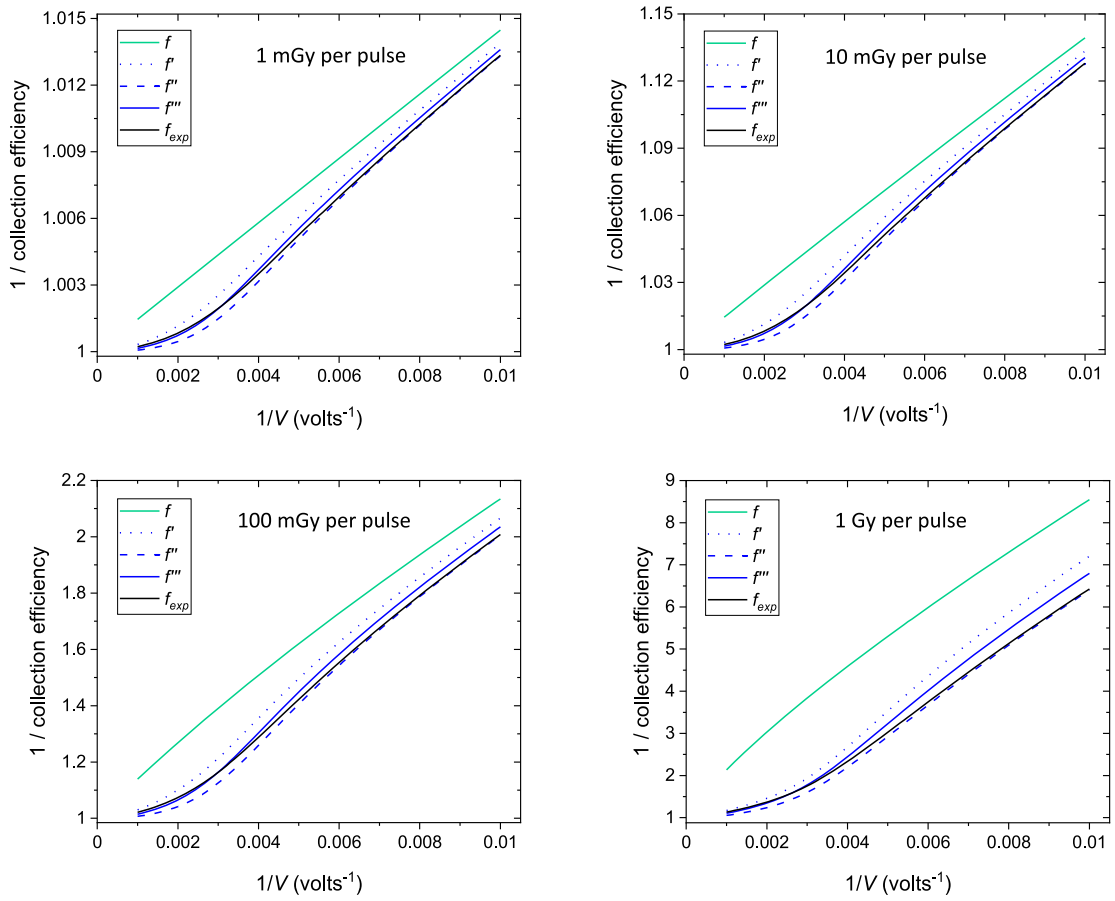

Figure 4. Jaffé plots corresponding to those in figure 3 for a parallel plate ionization chamber with a 2 mm gap between electrodes.

4. Discussion

A collection efficiency formula, f_{exp}, has been obtained by analytically solving the model of Boag *et al* (1996) which describes ion transport and recombination in parallel plate ionization chambers and allows for free electron effects. Because the derivation of f_{exp} is quite lengthy the formula was independently checked by running an in-house ion transport and recombination code, producing collection efficiency values in very close agreement with those obtained from f_{exp}.

Across the ($u = 0.01$–0.50, $p = 0$–0.60) range of chamber properties studied by Boag *et al* (1996), the maximum relative difference between collection efficiency values calculated using three approximate formulae obtained in the 1996 publication is 5.1%. Values of the approximate formula f''' lie closest to those of f_{exp} over much of the (u, p) range studied, although for $p \leqslant 0.2$ values of f'' are closer to f_{exp}. The greatest difference between f''' and f_{exp} is 0.78% relative. Given access to tabulated exponential integral values f_{exp} can easily be evaluated using a hand calculator, and since f_{exp} represents an exact solution of the model of Boag *et al* its use should reduce some of the ambiguity introduced into collection efficiency estimation by the multiple approximate formulae.

Greater differences between collection efficiencies calculated using the various formulae can be seen in figures 3 and 4, because the graphs in the figures effectively extend to higher u values than those of table 2. In the graphs the largest difference between correction factors based on f''' and f_{exp} is some 6.1% relative. For chamber potential differences above 200 V, f''' values are closest to the exact f_{exp} values. However, at 100 V with an electrode separation of 1 mm, f'' is closest to f_{exp} and this is also the case at 100–200 V with a separation of 2 mm. These voltages and electrode separations correspond to p values of 0.026–0.163.

The model of Boag *et al* (1996) ignores electric field distortions resulting from imbalances between the spatial distributions of positive and negative charges, an effect that becomes substantial at doses-per-fraction $\geqslant$100 mGy. Consequently, while f_{exp} represents an exact solution of the model, like the approximate collection efficiency formulae it does not account for field distortion effects at very high doses-per-pulse.

The approach used to derive f_{exp} is more intricate than the method used by Boag (1950) and Boag *et al* (1996) to obtain the f, f', f'' *and* f''' formulae, but accounts exactly for evolving ion cloud non-uniformity during

transport. It would be useful to further extend this analytical approach to include spatial variations in the electric field-strength and drift velocities of free electrons and ions. This is challenging but would potentially allow collection efficiency formulae to be obtained for cylindrical ionization chambers in which electric fields are intrinsically non-uniform.

If the effects of electric field non-uniformities could be described using analytical methods, it might also be possible to include in the analysis changes in the field due to evolving imbalances in charge distributions. This would perhaps allow a closed-form collection efficiency formula to be obtained that accounts for free electron effects, electric field non-uniformity and field distortion at high doses-per-pulse. Such a formula would provide further insights into how the various transport and recombination factors collectively influence detector performance when electric field distortion is substantial. It could also be used to calculate collection efficiency values for this circumstance faster and more conveniently than by running computational transport codes (Gotz *et al* 2017, Kranzer *et al* 2021).

5. Conclusions

A collection efficiency formula f_{exp} has been derived, based on an exact solution of the model of Boag *et al* (1996) which describes recombination in parallel plate ionization chambers and includes free electron effects but excludes electric field distortion. Calculated values of f_{exp} are in excellent agreement with collection efficiencies obtained computationally using an ion transport and recombination code.

Of the three approximate collection efficiency formulae developed by Boag *et al* (1996) values of f''' most often lie closest to the exact f_{exp} values, although when only 10%–20% of free electrons reach the anode, f'' rather than f''' values lie closest to f_{exp}. Over the ($u = 0.01$–0.50, $p = 0$–0.6) range studied by Boag *et al* (1996), the maximum relative difference between f''' and f_{exp} is 0.78%. For larger u values corresponding to doses per pulse of 100 and 1000 mGy and an electrode separation of 2 mm, maximum relative differences between correction factors based on f''' and f_{exp} reach 1.5% and 6.1% respectively.

Use of the exact f_{exp} formula should reduce ambiguities in collection efficiency estimates currently obtained from three different approximate formulae. It must be remembered, though, that like the approximate formulae, f_{exp} does not account for electric field distortion which becomes substantial at doses-per-pulse $\geqslant$100 mGy.

Appendix

Consider an air-filled plane-parallel ionization chamber with the geometry shown in figure A1. Denote by $t = 0$ an early time after a pulse of radiation, when a fraction $p = (1 - \exp(-ad))/(ad)$ of the free electrons initially liberated have been collected, the rest have formed negative ions, and no ions have yet moved significantly. At this time the densities of the positive and negative ions in the chamber are respectively

$$n_+(\hat{x},\, t = 0) = n_0,\;\; n_-(\hat{x},\, t = 0) = n_0\,(1 - \exp(-a\hat{x})). \tag{A1}$$

In equation (A1) n_0 is the uniform density of positive ions initially generated by the radiation pulse and $\hat{x}$ is distance to the right of the cathode in the rest-frame of the chamber.

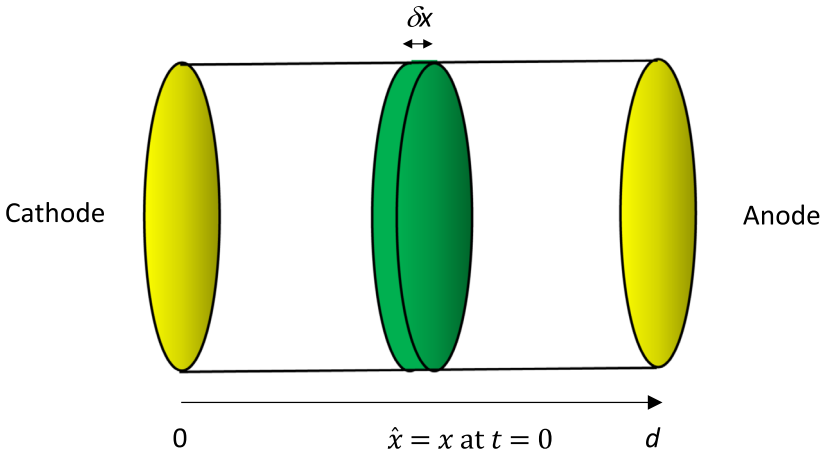

Figure A1. A schematic illustration of the cavity of a plane parallel ionization chamber showing in gold the cathode and anode separated by a distance d, and in green a slab of negative charge of thickness δx. In the rest-frame of the detector the cathode and anode have $\hat{x}$-coordinates 0 and d and the green slab is initially located at $\hat{x}$. In the rest-frame of the positive ions the electrodes have x coordinates that at time $t = 0$ are also 0 and d, and the position x of the slab in this rest-frame also equals $\hat{x}$ at this time. In real detectors the cavity thickness d is less than the diameter of the electrodes.

In the absence of a net flow of ions into or out of a small region, the densities of both positively and negatively charged ions in the region decrease at a rate $\alpha n_+ n_-$ where α is the recombination rate-constant. From this it is possible to calculate charge recombination for positive and negative ions as they move past each other, travelling to the cathode and anode respectively with velocities v_+ and v_-. For ease of analysis, in the rest of the appendix the rest-frame is shifted to one in which the positive ions have zero velocity and the negative ions move past them to the right with speed $v_{\text{tot}} = (v_+ + v_-)$. Locations in the shifted frame are denoted by x rather than $\hat{x}$, and the origins $\hat{x} = 0$ and $x = 0$ are coincident at $t = 0$.

Now focus on a thin slab of negative ions initially located at $x \rightarrow x + \delta x$ as it moves to the right (figure A1). Denote as $n_{-x}(t)$ the density of negative ions remaining in the slab at time t, when the slab is at $x + v_{\text{tot}} t$. Throughout the appendix $n_{\pm}(x,\ t)$ is used to describe the density of positive or negative ions at position x at time t, whereas $n_{\pm x}(t)$ describes density at time t in a thin slab that was located at x when $t = 0$. Consequently $n_{\pm}(x,\ t)$ and $n_{\pm x}(t)$ are different quantities but equivalent at $t = 0$.

The rate of change of $n_{-x}(t)$ is

$$dn_{-x}(t)/dt = -\alpha\, n_{-x}(t) n_+(x + v_{\text{tot}} t,\ t), \tag{A2}$$

and integrating (A2) leads to

$$\frac{n_{-x}(t)}{n_{-x}(0)} = \exp\left(-\alpha \int_0^t n_+(x + v_{\text{tot}} t',\ t')\right) dt'. \tag{A3}$$

Setting the upper time-limit to $\tau_x = (d - x)/v_{\text{tot}}$, at which point the slab has passed right through the cloud of positive ions initially to its right in the chamber, and changing variable to $y = x + v_{\text{tot}} t'$, equation (A3) becomes

$$\frac{n_{-x}(\tau_x)}{n_{-x}(0)} = \exp\left(-\frac{\alpha}{v_{tot}} \int_x^d n_+(y,\ t = (y - x)/v_{\text{tot}})\right) dy = \exp\left(-\frac{\alpha}{v_{\text{tot}}} N_{+x}\right), \tag{A4}$$

where

$$N_{+x} = \int_x^d n_+(y,\ t = (y - x)/v_{\text{tot}})\, dy, \tag{A5}$$

is the total number of positive ions per area passed through by the slab initially located at x. Thus, the number of recombination events that occur per unit area as the thin slab of negative charge passes completely through the cloud of positive ions to its right is

$$\delta R_x = \delta\, x(n_{-x}(0) - n_{-x}(\tau_x)) = \delta x\, n_{-x}(0) \left[1 - \exp\left(-\frac{\alpha}{v_{\text{tot}}} N_{+x}\right)\right]. \tag{A6}$$

Defining R_x as the total number of recombinations per area after all the slabs initially located between 0 and x pass completely through the positive ions to their right, then

$$R_x = \int_0^x (dR_{x'}/dx')\, dx' , \tag{A7}$$

where

$$\frac{dR_x}{dx} = n_{-x}(0) \left[1 - \exp\left(-\frac{\alpha}{v_{\text{tot}}} N_{+x}\right)\right]. \tag{A8}$$

Now, denote as $N_+(x,\ 0)$ the total number of positive ions per area that are initially positioned to the right of x at time $t = 0$

$$N_+(x,\ 0) = \int_x^d n_+(y,\ t = 0)\, dy, \tag{A9}$$

then

$$N_+(x,\ 0) - N_{+x} = \tilde{R}_x, \tag{A10}$$

where $\tilde{R}_x$ is the total number of positive charges per area initially lying to the right of x that have already recombined with negative ions before the slab originally located at x travels through them. These recombination events are due to the negative ions located to the right of the slab having moved through the positive charge cloud ahead of the slab, and consequently $\tilde{R}_x$ is given by

$$\tilde{R}_x = \int_x^d (dR_{x'}/dx')\, dx'. \tag{A11}$$

From equations (A7), (A8), (A10) and (A11)

$$\begin{aligned} d\widetilde{R}_x/dx &= -dR_x/dx = -n_{-x}(0)\left[1 - \exp\left(-\tfrac{\alpha}{v_{\text{tot}}}N_{+x}\right)\right] \\ &= -n_{-x}(0)\left[1 - \exp\left(-\tfrac{\alpha}{v_{\text{tot}}}(N_+(x,0) - \widetilde{R}_x)\right)\right], \end{aligned} \tag{A12}$$

$\tilde{R}_x$ is also given by

$$\tilde{R}_x = N_-(x,0) - \tilde{C}_x = \int_x^d n_-(x',0)dx' - \tilde{C}_x, \tag{A13}$$

in which $N_-(x,0)$ is the total number of negative ions per unit area located to the right of x at time zero, and $\tilde{C}_x$ is the number of these negative ions per area that pass through the positive ions and are collected at the anode. Differentiating equation (A13) with respect to x and comparing with (A12)

$$-n_-(x,0) - d\widetilde{C}_x/dx = -n_{-x}(0)\left[1 - \exp\left(-\frac{\alpha}{v_{\text{tot}}}(N_+(x,0) - \widetilde{R}_x)\right)\right], \tag{A14}$$

or

$$d\widetilde{C}_x/dx = -n_{-x}(0)\exp\left(-\frac{\alpha}{v_{\text{tot}}}(N_+(x,0) - N_-(x,0) + \widetilde{C}_x)\right). \tag{A15}$$

Defining

$$g(x) = n_{-x}(0)\exp\left(-\frac{\alpha}{v_{\text{tot}}}(N_+(x,0) - N_-(x,0))\right). \tag{A16}$$

Equation (A15) can be written as

$$d\widetilde{C}_x/dx = -\exp\left(-\frac{\alpha}{v_{\text{tot}}}\widetilde{C}_x\right)g(x). \tag{A17}$$

Changing variable to $m(x) = \exp\left(-\frac{\alpha}{v_{\text{tot}}}\widetilde{C}_x\right)$

$$d\widetilde{C}_x/dx = \left(\frac{-v_{\text{tot}}}{\alpha m(x)}\right)dm/dx, \tag{A18}$$

and substituting this in (A17)

$$dm/m^2 = \frac{\alpha}{v_{\text{tot}}}g(x)dx, \tag{A19}$$

which integrates between limits x_1 and x_2 to

$$[-1/m]_{x_1}^{x_2} = \left[-\exp\left(\frac{\alpha}{v_{\text{tot}}}\widetilde{C}_x\right)\right]_{x_1}^{x_2} = \frac{\alpha}{v_{\text{tot}}}\int_{x_1}^{x_2} g(x)dx. \tag{A20}$$

Setting x_1 to 0 and x_2 to d

$$\exp\left(\frac{\alpha}{v_{\text{tot}}}\widetilde{C}_0\right) - \exp\left(\frac{\alpha}{v_{\text{tot}}}\widetilde{C}_d\right) = \exp\left(\frac{\alpha}{v_{\text{tot}}}\widetilde{C}_0\right) - 1 = \frac{\alpha}{v_{\text{tot}}}\int_0^d g(x)dx, \tag{A21}$$

or

$$\widetilde{C}_0 = \frac{v_{\text{tot}}}{\alpha}\ln\left(1 + \frac{\alpha}{v_{\text{tot}}}\int_0^d g(x)dx\right), \tag{A22}$$

where $\tilde{C}_d$ describes the number of negative ions per area collected at the anode that were initially located to the right of d, and is zero since this range of locations lies outside the region between the electrodes. $\tilde{C}_0$ is the total number of negative ions per area that eventually arrive at the anode regardless of their original x position in the chamber, and together with the known number of free electrons per area collected at the anode it defines the total negative charge collected per unit cross-sectional area. To evaluate $\tilde{C}_0$, all that remains is to solve the integral

$$I = \int_0^d g(x)dx = \int_0^d n_{-x}(0)\exp\left(-\frac{\alpha}{v_{\text{tot}}}(N_+(x,\,0) - N_-(x,\,0))\right)dx, \tag{A23}$$

in which $n_{-x}(0)$ equals $n_0(1 - \exp(-ax))$ (equation (A2)), $N_+(x,\,0)$ is obtained by integrating $n_+(x,\ t = 0)$ (equations (A1) and (A9))

$$N_+(x,\,0) = n_0(d - x), \tag{A24}$$

and $N_-(x,\,0)$ is likewise obtained by integrating $n_-(x,\ t = 0)$

$$N_-(x,\,0) = n_0(d - x) - (n_0/a)\,(\exp(-ax) - \exp(-ad)). \tag{A25}$$

Substituting these quantities into equation (A23), I can be written as

$$I = B\int_0^d (1 - \exp(-ax))\exp(-A\exp(-ax))\,dx, \tag{A26}$$

where

$$A = n_0/(v_{\text{tot}}a) \text{ and } B = n_0\exp(A\exp(-ad)). \tag{A27}$$

Splitting this as

$$\begin{aligned} I &= I_1 + I_2 \\ I_1 &= B\int_0^d \exp(-A\exp(-ax))\,dx \\ I_2 &= -B\int_0^d \exp(-ax)\exp(-A\exp(-ax))dx, \end{aligned} \tag{A28}$$

then

$$I_2 = -\frac{B}{aA}[\exp(-A\exp(-ax))]_0^d. \tag{A29}$$

Changing variable to $w = A\exp(-ax)$

$$I_1 = \frac{B}{a}\int_{A\exp(-ad)}^{A} \frac{\exp(-w)}{w}\,dw \tag{A30}$$

$$= \frac{B}{a}[E_1(A\exp(-ax))]_0^d, \tag{A31}$$

where E_1 is the standard exponential integral function, defined as

$$E_1(\zeta) = \int_\zeta^\infty \frac{\exp(-\zeta')}{\zeta'}d\zeta'. \tag{A32}$$

Substituting $I = I_1 + I_2$ back into equation (A22) leads to

$$\widetilde{C}_0 = \frac{v_{\text{tot}}}{\alpha}\ln\left(1 + \frac{\alpha}{v_{\text{tot}}}\frac{B}{a}\left[E_1(A\exp(-ax)) - \frac{\exp(-A\exp(-ax))}{A}\right]_0^d\right). \tag{A33}$$

The collection efficiency, f, of the ionization chamber is the sum of the total numbers of free electrons and negative ions collected per unit cross-sectional area, divided by $n_0 d$, the total number of electrons (or positive ions) initially generated per area. Therefore

$$\begin{aligned} f = \frac{pn_0d + \widetilde{C}_0}{n_0d} = p + \frac{v_{\text{tot}}}{\alpha n_0 d}\ln\Bigg(1 + \frac{\alpha}{v_{\text{tot}}}\frac{B}{a}[E_1(A\exp(-ax)) \\ - \frac{\exp(-A\exp(-ax))}{A}]_0^d\Bigg). \end{aligned} \tag{A34}$$

Putting A and B from equation (A27) into (A34) gives

$$f = p + \frac{v_{\text{tot}}}{\alpha n_0 d}\ln\left(\begin{array}{l} 1 + \frac{\alpha n_0}{av_{tot}}\exp\left(\frac{n_0}{av_{tot}}\exp(-ad)\right) \\ \times\left[E_1\left(\frac{\alpha n_0}{av_{\text{tot}}}\exp(-ax)\right) - \frac{\exp\left(-\frac{\alpha n_0}{av_{\text{tot}}}\exp(-ax)\right)}{\frac{\alpha n_0}{av_{\text{tot}}}}\right]_0^d \end{array}\right). \tag{A35}$$

The velocities of positive and negative ions can be written in terms of their mobilities k_1 and k_2 and the electrical field in the cavity, equal to the potential difference between the electrodes, V, divided by d (Boag *et al* 1996)

$$v_{tot} = v_+ + v_- = (k_1 + k_2)V/d, \tag{A36}$$

and substituting this into (A35) yields

$$f = p + \frac{1}{u}\ln\left(1 + \frac{u}{ad}\exp\left(\frac{u}{ad}\exp(-ad)\right)\right.$$
$$\left.\times\left[E_1\left(\frac{u}{ad}\exp(-ax)\right) - \frac{\exp\left(-\frac{u}{ad}\exp(-ax)\right)}{\frac{u}{ad}}\right]_0^d\right), \tag{A37}$$

where

$$u = \frac{\alpha n_0 d^2}{(k_1 + k_2)V}. \tag{A38}$$

When the second term in the square bracket in (A37) is evaluated at the upper limit of d it cancels the 1 at the start of the logarithm and the equation simplifies to

$$f = p + \tfrac{1}{u}\ln\left(\tfrac{u}{ad}\exp\left(\tfrac{u}{ad}\exp(-ad)\right)\right.$$
$$\left.\times\left\{E_1\left(\tfrac{u}{ad}\exp(-ad)\right) - E_1\left(\tfrac{u}{ad}\right) + \frac{\exp\left(-\frac{u}{ad}\right)}{\frac{u}{ad}}\right\}\right), \tag{A39}$$

From equation (1)

$$\frac{u}{ad}\exp(-ad) = \frac{u}{ad} - up, \tag{A40}$$

which allows (A39) to be re-written as

$$f = p + \frac{1}{u}\ln\left(\frac{u}{ad}\exp\left(\frac{u}{ad} - up\right)\right.$$
$$\left.\times\left\{E_1\left(\frac{u}{ad}\exp(-ad)\right) - E_1\left(\frac{u}{ad}\right) + \frac{\exp\left(-\frac{u}{ad}\right)}{\frac{u}{ad}}\right\}\right). \tag{A41}$$

Finally, by extracting the factor $\exp(-up)$ from inside the logarithm, a constant term $-p$ is added outside it cancelling the $+p$ term, and the equation becomes

$$f = \frac{1}{u}\ln(1 + R\exp(R)[E_1(R\exp(-ad)) - E_1(R)]), \tag{A42}$$

where $R = u/(ad)$.

References

Boag J W 1950 Ionization measurements at very high intensity *Br. J. Radiol.* **23** 601–11

Boag J W, Hochhäuser E and Balk O A 1996 The effect of free-electron collection on the recombination correction to ionization measurements of pulsed radiation *Phys. Med. Biol.* **41** 885–97

Boutillon M and Perroche-Roux A M 1987 Re-evaluation of the W value for electrons in dry air *Phys. Med. Biol.* **32** 213–9

Christensen J B, Tölli H and Bassler N 2016 A general algorithm for calculation of recombination losses inionization chambers exposed to ion beams *Med. Phys.* **43** 5484–92

Di Martino F, Gianelli M, Traino A C and Lazzeri M 2005 Ion recombination correction for very high dose-per-pulse high-energy electron beams *Med. Phys.* **32** 2204–10

Gotz M, Karsch L and Pawelke J 2017 A new model for volume recombination in plane-parallel chambers in pulsed fields of high dose-per-pulse *Phys. Med. Biol.* **62** 8634–54

Gradshteyn I S and Ryzhik I M 2007 *Table of Integrals, Series and Products* ed A Jeffrey and D Zwillinger (Burlington, MA: Academic) 7th edn pp 883–5

Jaffé G 1913 Zur theorie der ionisation in kolonnen *Ann. Phys.* **347** 303–44

Jaffé G 1929 Zur theorie der ionisation in kolonnen. II *Ann. Phys.* **393** 977–1008

Kanne W and Bearden J 1936 Columnar ionization *Phys. Rev.* **50** 935–8

Kranzer R, Poppinga D, Weidner J, Schüller A, Hackel T, Looe H K and Poppe B 2021 Ion collection efficiency of ionization chambers in ultra-high dose-per-pulse electron beams *Med. Phys.* **48** 819–30

Laitano R F, Guerra A S, Pimpinella M, Caporali C and Petrucci A 2006 Charge collection efficiency in ionization chambers exposed to electron beams with high dose per pulse *Phys. Med. Biol.* **51** 6419–36

McManus M, Romano F, Le N D, Farabolini W, Giardi A, Royle G, Palmans H and Subiel A 2020 The challenge of ionisation chamber dosimetry in ultra-short pulsed high dose-rate Very High Energy Electron beams *Sci. Rep.* **10** 9089

Petersson K, Jaccard M, Germond J-F, Buchillier T and Bochud F 2017 High dose-per-pulse electron beam dosimetry—A model to correct for the ion recombination in the Advanced Markus ionization chamber *Med. Phys.* **44** 1157–67

Thomson J J and Thomson G P 1928 *Conduction of Electricity Through Gases* vol 1 (Cambridge: Cambridge University Press) pp 137–8